Jurnal Teknologi

Full Paper

RETROFITTING OF SELF COMPACTING RC HALF JOINTS WITH INTERNAL DEFICIENCIES BY CFRP FABRICS

Qasim M. Shakir*, Baneen B. Abd

Department of Civil Engineering, University of Kufa, Najaf, Airport Street, Iraq

Article history
Received
20 November 2019
Received in revised form
15 June 2020
Accepted
15 July 2020
Published online
27 October 2020

*Corresponding author
qasimm.alabbasi@uokufa.edu.iq

Graphical abstract

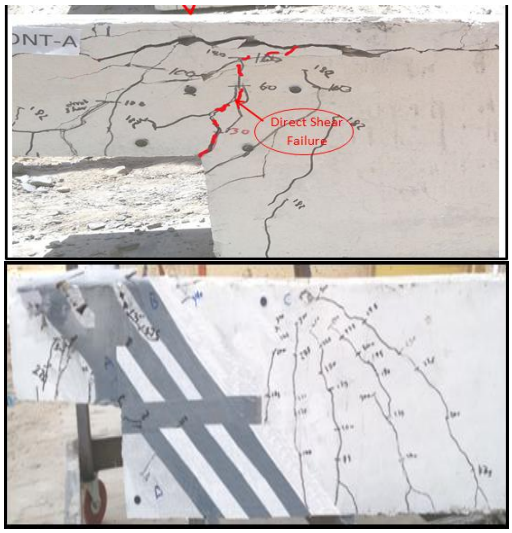

Abstract

An experimental study has been conducted to scrutinize the response of reinforced self-compacting concrete half joints upgraded with CFRP strips. Fourteen RC half joints have been tested. Two values of shear slenderness ratio were considered, namely 1.5 and 1.0. Two beams have been treated as reference specimens (with the design steel), and the twelve other beams were casted with deficiency in steel of the hanger and the extended end regions relative to the control beams. Eight of these beams have been strengthened with different arrangements to discuss the influence of shear slenderness ratio and strengthening arrangement on the overall performance of such joint elements. It is found that the reduction in nib-main steel by about 50% results in decreasing load capacity by about 36% and 15% for shear slenderness ratio of 1.5 and 1.0 respectively. Also, it is found that the orthogonal arrangement combined with inclined strips yielded the best results in terms of preventing the diagonal shear failure at the re-entrant corner with maximum enhancement in load capacity by 18%. In addition, the maximum improvement in failure load when strengthening hanger region by such alignment was about 23%. Results also revealed that the effective stiffness and ductility ratio enhanced with reducing shear span of a half joint and may be adopted as a good indicator to evaluate the suitable strengthening scheme. Moreover, it is concluded that the relative displacement method for predicting the ductility ratio is more applicable than that based on the dissipated energy.

Keywords: Upgrading, self-compacting concrete, half joints, shear-slenderness ratio, CFRP sheets

1.0 INTRODUCTION

A precast structure is a reinforced concrete construction that is composed of several elements which are casted separately then assembled in site. Sometimes, parts of the structure as columns and beams are precasted. Then, beyond installation in site the slab is cast in place. Although precast construction has several advantages related with cost, quality of product and time needed for construction. It has some disadvantages caused by heavy weights of large members, difficulties in installation and increased flexibilty of the overall structure.

Precast structure are different from the cast-in-place one in which the elements are connected monolithically and steel reinforcement pass through the joints of the structure from a member to another. Consequently, the rigidity of such structures is relatively high if compared with precast construction

in which the forces are transferred through more flexible joints (connections) by bearing action and higher moments and deflection values are expected to be obtained. However, joints are needed in precast structures to reduce the size and weights of the elements to facilitate the delivery to the construction site. Thus, a considerable attention has been given to the detailing of the connections in precast structures to insure that forces are transferred safely and softly.

Several joints arrangements have been proposed to join elements in a precast structure, some of these are depicted in Figure 1, and are:

(1) beam supported by inverted T-girder.
(2) corbel-beam connection.
(3) two-half joints.

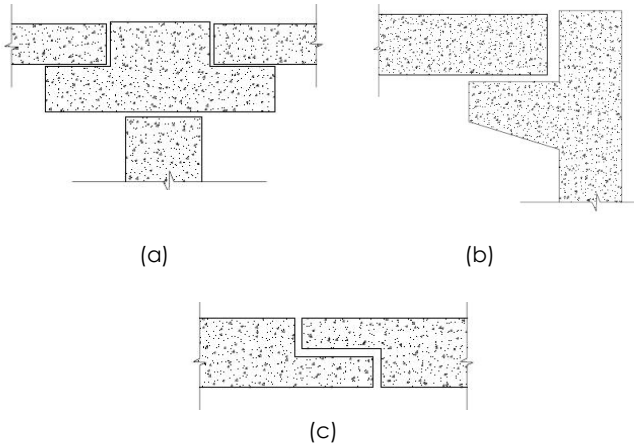

Figure 1 Type of the precast concrete joints (a) beam-inverted T-Girder (b)beam-corbel joint (c) half joints

Several previous studies used dapped ends at the tip of the precast beams [1-3] for several merits:

(1) The use of dapped ends results in increasing the lateral stability of the beam due to lowering its center of gravity.
(2) Reducing the total height of the structure. Thus, increase its lateral stability in addition to the economical view of using of construction materials.
(3) Better fabrication with corbels or cross beams can be obtained.
(4) In the half joints that consist of two dapped ends. The joint is located at inflection point (zero moment). Thus, the moment capacity may not be affected due to introducing the joint.

However, the inclusion of dapped end has several demerits, which are:

(1) Special attention should be given when analysis, design, delivery to construction site and installing.
(2) weak regions are generated at the re-entrant corner and the junction between the extended end and the beam.

Any structural member may be divided into two types of regions, B-regions at which the stress countourlines are distributed uniformly without considerable disturbance. In such regions the conventional bending theory can be used to study the behavior. The second type of regions is the D-regions, in which there is some disturbance of stress line exists. In general, the D-regions include corners or a concentrated point loads. Such zones restrict the unformed flow of stresses and act as points of stress concentration. Early studied stated the the dapped ends are one of the disturbed region (D-regions) that can not be designed by the well-known Bernoulli Theory [4].

Studies concerned the dapped ends may be divided into three groups. The first is interested by studying the behavior and establishing the theoretical approaches to analysis and design of dapped ends. The beginning of this stage back to the late of the sixties when Reynolds in 1969 proposed a simple procedure to design RC half-joints [5]. In 1979 Mattock and Chan [6] adopted the procedure suggested by Mattock *et al.* [7], that used for corbels to be applied on dapped ends. In 1984 Collins and Mitchell proposed a design approach for D-regions using STM models. Then, STM approach was adopted by in 2002 by ACI 318 code [8]. Barton *et al.* [9] calibrated the validity of the STM model against the PCI method and the Menon/Furlong design methods. Extensive studies have been conducted by several researchers to investigate variables that affect the performance of RC dapped ends including compressive strength of the concrete [10, 11], inclusion steel fibers [12, 13], dapped end dimensions [3, 14] and internal detailing of reinforcement in the disturbed zone [8, 15, 16]. The second domain of studies is focused on the utilizing the prestressing techniques to improve the response of dapped ends and half joints to control the propagation of the shear cracking. In 1973 Werner and Dilger [17] tested post-tensioned DEBs with combined loading and different dapped end arrangements. Then, successive studies have been published to investigate the variable including shape of dapped end, prestressing level, grade of concrete, detailing of HR, depth of the nib end, length of horizontal extension of HR, a/d ratio, using inclined bars in dapped end, ratio of horizontal/vertical loading [18-21].

Deficiencies in half joints has two types, external and internal. External deficiency which may be caused due to change in use, severe loading (as repeated, dynamic or cyclic loading) or deterioration of the structure due to severe conditions (as aggressive circumstances or elevated temperature effects) and internal which may rarely occurred due to the code differences, design errors and issues of steel arrangements. One of the earliest

studies that have been published in strengthening dapped ends have been achieved by Huang *et al.* [22] using externally bonded CFRP sheets. In 2005, Taher [23] studied the strengthening of deficient DEs with different techniques including unbounded inclined steel bolt anchored in pre-drilled hole, external steel plate jacketing, exterior CFRP sheets, exterior CFRP stripping and combination of carbon fiber wrapping and strapping. In 2012, Nagy-György *et al.* [24] discussed the adequacy of upgrading RC DEBs using EB CFRPs. In 2016, Atta and Taman [5] tested seven RC DEB that strengthened with different shapes of external prestressing technique directions: horizontal, vertical and inclined. Shakir and Alliwe [25] investigated experimentally the efficiency of using the NSM steel bars in strengthening the SCC RC dapped end regions with a/dd values of 1.0 and 1.5.

In this work, an experimental investigation have been achieved on fourteen half joints. The effect of shear slenderness ratio on cracking load, ultimate load and mode of failure was discussed in details. In addition, the range of influence of reduction in hanger and nib reinforcement have been investigated. Furthermore, using the externally installed, CFRP strips as a strengthening technique to retire the weakness in hanger and nib zones of the half joint have been studied. Several arrangement of the strips have been considered seeking for the best configuration that eliminated the weakness at half joint and the lack in reinforcement and allowed the half joint to behave as a non-dapped end beam. The performance is studied also, in terms of effective stiffness and ductility ratio. The present work established the bases to more advanced studies that considering dapped end beams with openings, vierendeel trusses with dapped ends, etc. Such beam are satisfying the sustainability aspects, strength, reduction the height of buildings, ease fabrication with corbels or cross inverted T- beams.

2.0 METHODOLOGY

An experimental observation has been achieved to investigate the effect of changing the shear span of the half joint of a half joint on the capacity of the half joint and the overall joint. Furthermore, the extent of efficiency of the external bonding technique using CFRP sheets to retire the load of capacity caused by some of deficiencies discussed in "introduction." Such deficiencies are proposed to occur with the hanger and extended end reinforcement. Several configurations have been proposed with the lowest quantity of CFRP (one layer).

Fourteen specimens have been tested under concentrated static load are grouped into two categories based on a/d value. Each group include one specimen with full reinforcement, one with reduced nib reinforcement, one with reduced hanger reinforcement, two with strengthened nib reinforcement and two with strengthened hanger reinforcement. The observation is based on studying the load deflection curve, cracking loads, failure load, cracking pattern, failure mode, energy dissipation up to failure (toughness), ductility ratio and effective stiffness.

2.1 Materials

The cube compressive strength of the self-compacting concrete used for casting the specimens tested in this work is 56 MPa. Several mixes have been tested to reach the optimal ratios of the constituent materials of the mix. The constituent materials used are ordinary Portland cement (Type I) that is tested based on IQ.S. 5/1984 [26], crashed stone with maximum size of 14 mm as coarse aggregate, natural sand as fine aggregate. Both coarse and fine aggregate are tested to confirm the requirements of IQS No.45/1984 [27]. Limestone powder is used as a low cost filler material to increase quantity of fines to improve the lubrication effect and slipping of aggregate particles. Then, enhancing workability and packing of particles. Consequently, reducing the hair cracking resulted from the excessive heat when cement hydration. Furthermore, increasing fines may eliminate the possibility of segregation of the mix materials. This may contribute in improving the compressive strength of concrete. The limestone powder is tested to confirm the requirements of the EFNARC [28]. Potable water is used for mixing and curing. Glinium 54 is used as a superplasticizer to increase the flowability and workability [29]. The reinforcing steel used consist of three sizes of deformed bars. The main longitudinal bars of the beam and the nib reinforcement (for the control specimen) are #16 bars mm. Bars of 10 or 12 are used as hanger reinforcement for the full reinforced specimens and deficiently reinforced hanger. The materials properties for steel bars are listed in Table 1. The tests were conducted according to ASTM A370-2005 specifications [30]. CFRP sheet strips type SikaWrap®-301C were used as strengthening materials. Such strips had 0.167 mm thickness, 50 mm widths and tensile strength of 4900 MPa [31]. The Sikadur-330 [32] epoxy based impregnating resin with tensile strength of 30 MPa is used with a ratio of 1A: 3B to fix CFRP strips on concrete surfaces.

Table 2 elucidates the proportions of the material constituent of the mix adopted in the present study.

Table 1 Properties of steel bars

Bar dia.(mm)	Φ 10	Φ12	Φ 16
Yield stress(MPa)	568	615	634
Ultimate strength(MPa)	726	712	748

Table 2 Proportion of concrete mix

Constituents Materials	Quantity/m^3
Cement (kg)	400
Fine Aggregate (kg)	962
Course Aggregate (kg)	780
Limestone Powder (kg)	75
Water (kg)	128.7
Water/ Cement Ratio	0.32
Superplasticizer (L)	4.8

2.2 Description of Specimens

For all specimens, the cross section dimensions were 200 mm width, 400 mm height, and the overall length was 1500 mm. The nib has a length of 250 mm and an overall depth of 200 mm. The specimens have been grouped into two categories, A with a/d=1.5 and B with a/d=1.0. In each set, three beams were investigated as a non-strengthened beams and other beams were strengthened with different arrangement of CRFP sheets. The dimensions and reinforcement details for a beam with full reinforcement are shown in Figure 2. The reinforcement quantities for the tested half joints for the hanger region and the extended (nib) end are listed in Table 3.

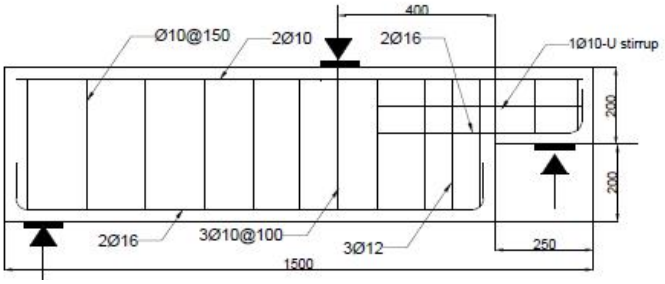

Figure 2 Details of reinforcement for the control specimens

Table 3 Reinforcement quantities for the tested half joints at hanger and nib end

	Control specimens	Specimens with Reduced hanger steel	Nib steel
Hanger steel	3#12	2#10	3#12
Nib steel	2#16	2#16	2#10

2.3 CFRP Strengthening Systems

CFRP strips can be externally bonded onto reinforced concrete surfaces in three forms, namely full sided wrapped (closed form), three sided wrapped (U-shaped), and two sides wrapped. The CFRP strips can be installed vertically, horizontal or inclined. The following procedure can be considered for externally bonded carbon fiber reinforced polymer:

1. Prepare the surface of the beam to be strengthened;
2. Apply epoxy to the prepared surfaces;
3. Install the CFRP laminates;
4. Allow the epoxy to cure

In the program of the study, the strengthening arrangement of the specimens are selected carefully depending on the results of the deficiently reinforced specimens. The control and beams with defects are tested first. The failure modes are determined and the history of development of cracks (cracking patterns) are traced and analyzed attentively. Then, the first model of strengthening is installed, tested and the results are analyzed, then the second strengthening scheme is proposed accordingly, and so on. The different arrangements for strengthening are detailed in Table 4.

Table 4 Characteristics of specimens

Designation	configuration description
CONT-A	Full reinforcement
HCONT-A	The HR is reduced by 50%
HSTR-1-A	3-strips with angle 45^0
HSTR-2-A	2-vertical U-shape in hanger and NE+ 2-horozotal strips at NE
NCONT-A	The NR is reduced by 60%
NSTR-1-A	L-shaped sheet, 1-layer
NSTR-2-A	L-shaped sheet, 1-layer + 2-horozotal sheet in each side
CONT-B	Full reinforcement
HCONT-B	The HR is reduced by 50%
HSTR-1-B	3-strips with angle 45^0
HSTR-2-B	2-vertical -U-shape at hanger and NE + 2-horozotal strips at NE
NCONT-B	The NR is reduced by 60%
NSTR-1-B	3-horizontal strips at NE+ 2-vertical U-shape at hanger
NSTR-2-B	3-horizontal strips at NE +3-strips at 45^0

NE: nib end; NR: main steel at nib; HR; hanger stirrups

3.0 RESULTS AND DISCUSSION

The results are discussed based on several performance indicators including loading history, cracking pattern, failure mode, failure load, effective stiffness, ductility ratio. Figure 3 shows the distribution of stresses in a loaded dapped end [33]. It can be seen that the stresses normal to the diagonal line from the re-entrant corner are tensile. This interprets why most of dapped end failed along this path. Moreover, it can be seen that the stresses at top fibers are in compression. Thus, the crushing or spalling of concrete occur at this level. Regard strengthening, several arrangements are suggested in this work. The diagonal to increase tension resistance across the diagonal crack. Vertical at hanger region, to substitute the lack in hanger steel and provide some tension resistance across the diagonal crack. Horizontal, to resist rotation of the

half joint part relative to the beam and resisting shear stresses also.

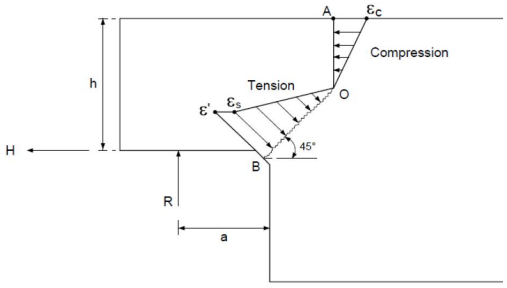

Figure 3 Strain distribution within critical path of failure [33]

Two values of a/d have been considered because it is needed to show the effect of shifting the support of the joints at which dapped end or half joint fabricated on the structural performance of the joint. In addition, it is intended to study the response of half joints where the shear force is dominant ($a/d \leq 1$) and the case when bending moment controls the behavior ($1< a/d \leq 2$). Sometimes the joint may be designed for small a/d but due to change in some requirement it become necessary to increase shear span and consequently increasing a/d ratio. In some cases support may shifted slightly due to some seismic loads, earthquake motions and explosive forces. Uncertainty of calculating the support position may result in changing the design and actual value of a/d value. Moreover, due to the thermal and environmental effects, it is needed to provide enough space to achieve the detailing of the expansion joints and that enough gap need to be provided to accommodate the expected movements due to change in temperature.

In all control beams, the first cracks initiated at the corner of half joint, while in the strengthened beams, the flexural shear crack was the first crack occurred at mid span of the beam with vertical or diagonal trend the point load. The cracking loads, ultimate load, failure modes and deflection at ultimate stages are listed in Table 5.

3.1 Control Specimens (CONT-A & CONT-B)

The recorded load-deflection results are depicted in Figure 4. It can be concluded that reducing a/d value from 1.5 to 1.0 results in increasing the failure load capacity by about 16.6%, higher stiffness and lower deflection of about 35.5%. Moreover, Figure 5 shows the cracking history for specimens CONT-A and CONT-B. It can be seen that the first crack for the specimen CONT-A, initiated at the re-entrant corner as a diagonal shear crack at load level of (40 kN). More cracks developed around the corner and within the D-region with further loading. As cracks developing away from re-entrant corner, it changes from being shear to flexural cracks. In addition, it is obvious that the crack emanated from the corner penetrates towards the compression face and tends to be horizontal.

For specimen CONT-B, first crack also initiated at the re-entrant corner as a diagonal shear type. With more loading, further cracks occurred around the corner and some at the extended end, the crack of the corner stagnated and another crack developed from the support with higher rate, influenced by the lack in shear force and increase in BM. This clarifies the effect of a/d (shear slenderness ratio) on the mode of failure. It can be seen that failure by the second mode is accompanied with higher degree of risk than the first one.

Table 5 Test results of specimens

beam	Pcs	Pcf	Pu	Δu	Mode
CONT-A	40	97	285	10.3	Diagonal shear-NE
HCONT-A	35	75	248	9.9	Diagonal shear-NE
HSTR-1-A	175	75	300	8.9	Diagonal shear-FS
HSTR-2-A	125	50	280	8.1	Diagonal shear-FS
NCONT-A	25	95	182	5.8	Direct shear-RE
NSTR-1-A	35	75	185	4.3	Rupture-CFRP
NSTR-2-A	50	80	200	3.8	Delamination-CFRP
CONT-B	50	100	300	7.4	Diagonal shear-RE
HCONT-B	25	70	262	7.1	Diagonal shear-NE
HSTR-1-B	120	75	340	6.4	Delamination-CFRP
HSTR-2-B	100	70	320	7.8	Rupture-CFRP
NCONT-B	20	90	255	7.25	Diagonal shear-NE
NSTR-1-B	80	70	295	6.9	Flexural- midspan
NSTR-2-B	100	75	300	5.6	Flexural- midspan

Pcs: shear crack load(KN); PCf: flexural crack load(KN); Pu: ultimate load(KN); Δu: maximum deflection(mm); Underlined: As observed; FS: far side(No-dap end); NE: nib end; RE: re-entrant corner

Bending moment (BM) has more influence with specimen CONT-A. Thus, the first crack initiated at the corner but the high value in bending moment and reduction in shear tend to shift the failure to be within the extended end in lieu the re-entrant corner. Thus, when a/d reduced, the mode of failure changed from diagonal tension failure in the extended end to diagonal tension failure at the re-entrant corner, as shown in Figure 6.

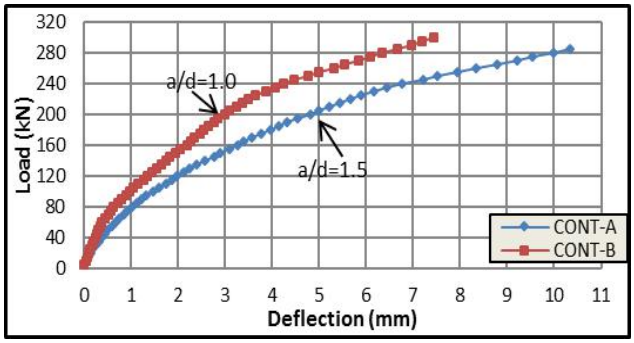

Figure 4 Loading history for specimens CONT-A &CONT-B

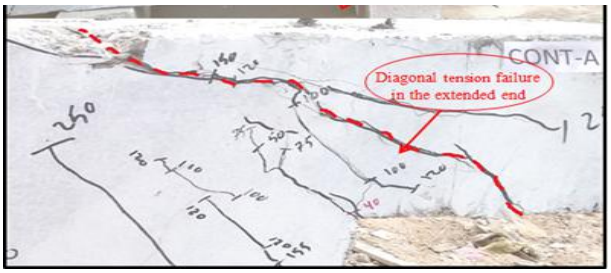

Figure 5 Loading history for specimens CONT-A

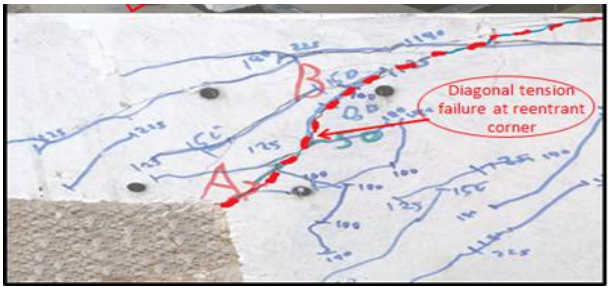

Figure 6 Loading history for specimens CONT-B

3.2 Specimens HCONT-A & HCONT-B

These specimens are tested to investigate the effect of the reduction in HR on the overall behavior of half joints. All the steel of the control specimens are kept constant expect that at HR were 2 Φ 10 mm stirrups were used (i.e. about 50% reduction). The reduction in hanger reinforcement may arise from different reasons including misunderstanding of the half-joint behavior and designing the stirrups of hanger zone based on the conventional shear design principles. Thus, reducing quantity of shear area by adopting larger spacing of stirrups. Consequently, increasing a/d value and reducing load capacity of half joint due to shifting the behavior to be controlled to be by moment rather of being controlled by shear force. In addition, the deficiency in the detailing of the bottom (CTT node) end or the top end (CCT node) of the hanger stirrups due to prior damage may affect the efficiency of the stirrups to resist tensile stresses at hanger zone. Moreover, the corrosion and lack of detailing of the longitudinal steel that represent one of the three forces of the equilibrium in the nodal point may result in violation of the equilibrium state. Change in use may result in increasing applied load and then the half joint support. Then, the hanger reinforcement may need to be retrofitted and increased to accommodate such excess of stresses and the half joint seems to be as deficiently reinforced hanger reinforcement.

It can be noticed from Figures 7 and 8 that the reduction in HR ratio results in a reduction in the failure load about 13% for both specimens.

Figures 9 and 10 show the cracking history for specimens HCONT-A, a/d=1.5 and HCONT-B, a/d=1.0. The effect of moment is more obvious and the compression force at the top fibers of the specimen HCONT-A is higher than for the specimen HCONT-B. Therefore, it is obvious that the crack emanating from the support starts with an angle of about 60° and tends to be horizontal gradually with loading progress.

This compressive force if not resisted by enough concrete block (as in low concrete compressive strength, and lightweight concrete) or by suitable steel, may result in spalling of the top layer and leading to a no prohibited sudden brittle failure. For the two specimens, it is clear that must of cracks propagated within the D-region referring to lack in tensile resistance in the vertical tie.

It is obvious that the reduction in hanger reinforcement results in a failure of the diagonal crack at the extended end and causes two different effects, reduction in tension force that maintain the two parts of the beam to work integrally, and reducing the shear resistance against the diagonal crack from the re-entrant corner. Thus, the fictitious support within the disturbed region will be softer and can be idealized as a hinge. Then, allowing to higher effect of the BM than the control beams. As a result, shifting the cracking plane to occur within the extended end rather than within the corner at which the first crack initiated. Then, inclination of failure plane for specimen HCONT-B was nearly constant of about 30° affected by shear at the re-entrant corner.

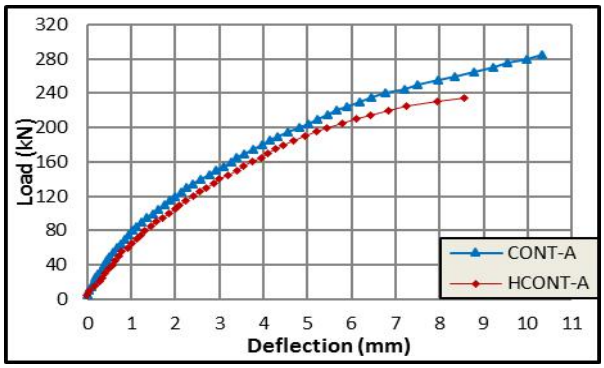

Figure 7 Loading history for specimens HCONT-A

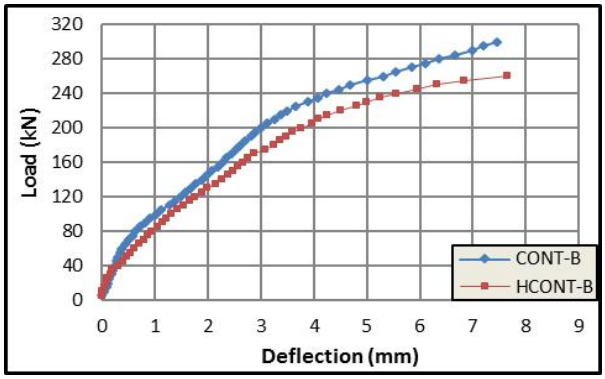

Figure 8 Loading history for specimens HCONT-B

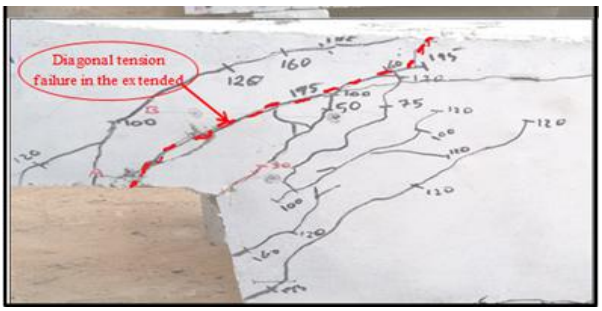

Figure 9 Loading history for specimens HCONT-A

Figure 10 Loading history for specimens HCONT-B

3.3 Specimens NCONT-A & NCONT-B

The deficiency in nib reinforcement may result from error in design caused by the lack of knowledge in the behavior of nib ends and consider all nib ends as cantilever beam. The error in applying the suitable method of design as using the shear-friction approach to design the half joint regardless of a/d ratio limits may lead to reduction in main reinforcement in the extended end. Damage due to severe environments or that the nib end may hit support severely due to improper installation procedure. Consequently, tip of the extended end may be prone to deterioration in the anchoring details of the main reinforcement. Change in use of the structure and change in the type of the load from being static to become as dynamic, cyclic, impact or seismic. All these effects may increase the stresses at the extended end and the behavior may become controlled by flexure rather than by shear force. Then, nib reinforcement become unable to resist the applied loads. Sometimes, the lack in the calculated bond length for the nib reinforcement may reduce to ability of the steel bars to resist the design load. Then, the nib end seems to be deficiently reinforced.

Figure 11 and 12 revealed that the reduction in NR led to a decrease in the failure load and deflection for a/d=1.5 of about 35.8% and 51.88%, respectively. Whereas for a/d=1, a reduction in the failure load and deflection 15% and 2.55% respectively.

Figures 13 and 14 show the cracking (history) patterns at failure for the two specimens. The reduction in tension force across the line between the re-entrant corner and point of load application play a major role in developing the failure plane in a high rate. Then, stabilizing of cracks developed towards the lower corner of the full depth beam accordingly. Also, the weakness of the half joint zone will stabilize and slow down of developing the flexural cracks within the region out of the disturbed zone. This difference being between levels of loading at which shear diagonal crack and flexural initiated i.e. 25 kN and 95 kN, for specimens NCONT-A & 20 kN and 90 kN for NCONT-B respectively. Furthermore, for specimen NCONT-A the first crack developed within the re-entrant corner grown vertically at junction towards the compression face. With further loading, new cracks developed and propagated mostly within the extended end.

For specimen NCONT-B, it can be seen that the first crack initiated at the re-entrant corner and cracks propagated around with more loading but the reduction in NR (nib reinforcement) results in increasing the effect of bending moment at a rate less than NCONT-A. Thus, crack that developed the failure plane shifted accordingly to the support reaction. In addition, the angle of crack is about 45° but when reaching the compression zone, the angle of crack became less due to the effect of the compressive force at the upper face. This can be explained as the lack of tension reinforcement within the extended end resulted in reducing the flexure resistance. In addition, increasing a/d value resulted in increasing bending moment. All these led to formation of crack of the flexure type. Moreover, due to the weakness and reduction in stiffness at the junction, Most of cracks will propagate at this region. Noticeable curvature at the junction occurred due to the lack of BM resistance. Thus, increasing the compression force at the top fibers, which increased with loading progress. For specimen NCONT-A, at load level of 182 kN, spalling at the top layers occurred. This resulted in a rapid failure, because it reduced the vertical path to be followed by flexure cracks. Regarding the intensity of cracks within the full depth beam, less number of cracks can be seen with adopting small (a/d) values.

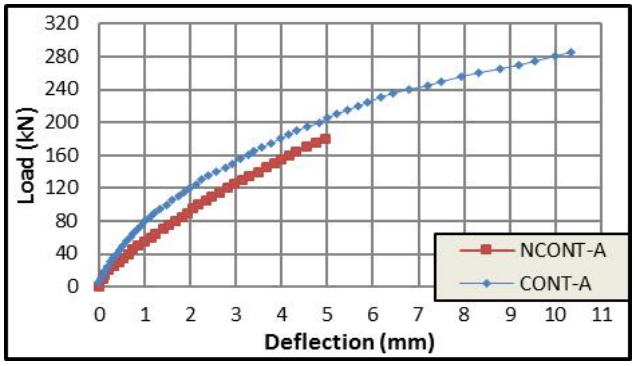

Figure 11 Loading history for Specimens NCONT-A

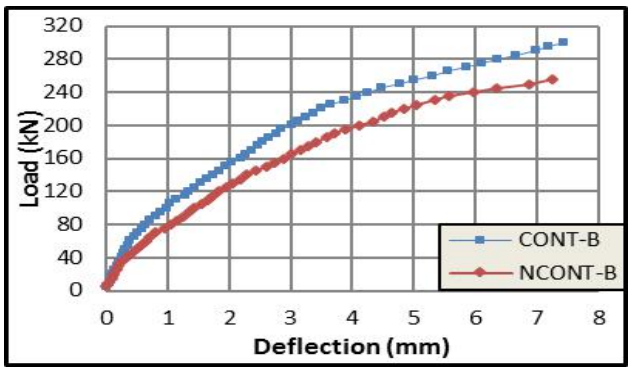

Figure 12 Loading history for specimens NCONT-B

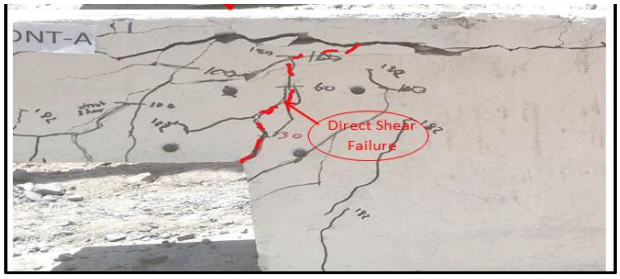

Figure 13 Cracks pattern for specimen NCONT-A

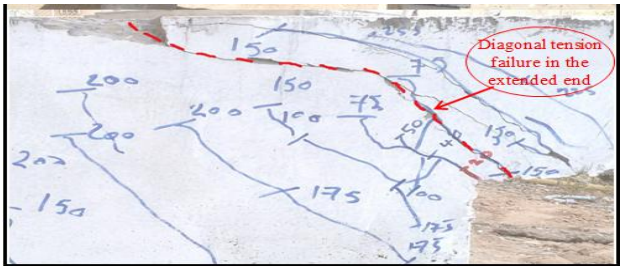

Figure 14 Crack pattern for specimen NCONT-B

3.4 Specimens HSTR1-A & HSTR2-A

Figure 15 shows the load deflection-curve obtained for the two strengthened specimens against the specimen HCONT-A. It can be seen that the specimen HSTR1-A yielded stiffer response and higher load than the HSTR2-A, i.e. an increment in the failure load capacity for specimens HSTR1-A and HSTR2-A of 17.33% and 11.43% with respect to HCONT-A, respectively.

Previous studies (Liem, 1983) showed that using inclined hanger reinforcement instead of the conventional vertical stirrups in the detailing of the internal reinforcements of the half joint members may improve the performance of such elements significantly. This conclusion has been utilized in the present work to improve the response of the definitely hanger reinforced half joints with large a/d values (1.5). Adding the inclined reinforcing elements that may interrupt the diagonal cracking initiated from the re-entrant corner and then arrest development of such crack and reduce the rate of crack propagation.

Comparing failure modes of specimens HSTR-1 and CONT-A and putting in mind that in specimen CONT-A provided with full reinforcement whereas specimen HSTR-A included reduced hanger reinforcement. Specimen CONT-A failed with the diagonal cracking at the extended end due to the large value of a/d =1.5. While specimen HSRT-1 failed by a mode similar to diagonal cracking for deep beams and the crack occurred beyond the point of load application (out of the disturbed zone). It can be seen that using the inclined strips resulted in significant enhancement of the response of the disturbed region. Small number of cracks initiated within the strengthened zone. Furthermore, no diagonal cracks from the re-entrant corner occurred nor at the extended end. The first developed crack from tension face towards point of load application is of the flexural type and it is vertically oriented. Further loading resulted in more crack to occur away from the upgraded half joint, Figure 16. When reaching the weak region, a diagonal cracks that are initiated from the far side of the specimen developed quickly and resulting in failure of the specimen. Thus, it is expected that using full shear reinforcement at this region may improve capacity considerably. The crushing at the top face around the point load refers to the high strength of the extended end that resisted curvature of the beam then, developing more capacity. Table 5 shows that this arrangement could retire efficiently the capacity of the full reinforced half joint with a ratio of (300/285) with lower deflection at failure of (8.9/10.3) compared to the specimen CONT-A.

For specimen HSTR2-A, it can be seen that the first crack initiated at the re-entrant corner at a load level less slightly than 125 kN, Figure 17. This reveals that the strengthening scheme HSTR1-A is more effective than scheme HSTR2-A. With further loading, some of cracks developed around this point but with less number and lengths if compared with the non-strengthened specimen HCONT-A.

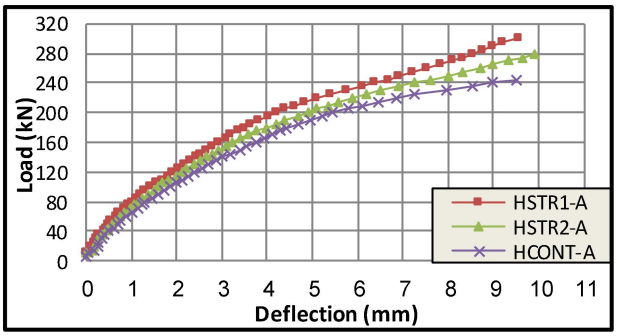

Figure 15 Effect of strengthening of hanger region (a/d=1.5)

Figure 16 Cracks patterns for strengthening beams HSTR1-A

Figure 17 Cracks patterns for strengthening beams HSTR2-A

In addition, some cracks are developed out of the strengthened region in the form of flexural crack. One of the diagonal cracks emanating at the far part from the nib end within load level close to that of the previous scheme. Thus, it is expected that if the deep beam action zone was reinforced adequately, then the failure load may be the same ratio of the cracking load (175/125).

Comparing the crack patterns for specimens HSTR1-A and HSTR2-A with the specimen HCONT-A, it can be seen almost few cracks formed in the extended end and hanger regions and most of cracks are shifted away from the strengthened zone. Also, a change in failure mode to diagonal shear failure at the deep beam action zone while it was diagonal tension failure in the extended end for beam HCONT-A. This may be due to the presence the CFRP sheets which results in shifting cracks far away towards the mid span of the beam.

It can be observed that the cracks near the strengthened region widened slightly and propagated away from the loading point, then grow rapidly leading to failure of specimens. It obviously can be concluded that more load capacity could be recorded, if it is designed efficiently using stirrups in the deep beam action zone of the beam.

Sometime, there is no enough space to provide the required bond length for the CFRP sheets because of the overtopping slab. Such problem can be solved by different mains such as enrolling the ends of the sheet on steel bars that to be embedded in groove partially filled with epoxy and made close to the bottom edge of the slab. Suitable types of epoxy need to be used at contact surface of different materials. Another method can be used by introducing holes within the body of the slab and passing the CFRP sheets throughout the holes that filled with epoxy. Then, fixing the sheets on the top face of the slab.

3.5 Specimens HSTR1-B & HSTR2-B

The same strengthening configurations used for specimens HSTR1-A & HSTR2-A are used to upgrade specimens with a/d=1. Compared to specimen HCONT-B, it can be noticed that the failure load was increased of about 23.23% and 18.43%, respectively, as shown in Figure 18.

Figure 19 shows the cracking pattern for the specimen HSTR1-B. It reveals that the first crack initiated as flexural crack at load level (75) and the first shear crack initiated at the re-entrant corner at load level of 120 kN. This may be because that effect of shear at the early stages is the dominant with smaller a/d value but with loading progress curvature increased and the effect of CFRP restricted cracking growth increase accordingly. Thus, few cracks penetrated through the strengthened zone as in HSTR1-A. Most cracks developed near the mid-span (non-strengthened zone) with cracking width smaller than the case in specimen HSTR1-A. It is suggested to provide more bond strength when strengthening half joint with smaller a/d values. The same configuration for the specimen HSTR2-A was adopted to be used in specimen HSTR2-B. However, due to its relatively high stiffness the DE resisted higher loads up to a load level of 340 kN when a bond failure between CFRP and concrete occurred which terminated the test. Thus, it is expected that the specimen may yield more capacity if this secondary failure is avoided. Regarding the cracks patterns the two, few cracks were observed in the extended end and hanger regions, and cracks did not penetrate through the CFRP sheets. Thus, led to a shifting of cracks away from the strengthened region and the failure of the strengthened specimens occurred due to rupture of the CFRP sheets, as shown in Figures 19 and 20.

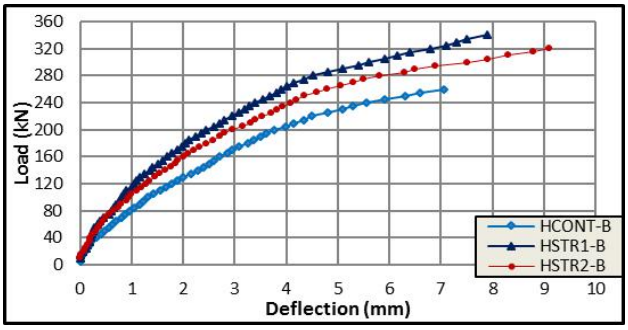

Figure 18 Effect of strengthening of hanger region (a/d=1.0)

Figure 19 Cracks patterns for strengthening beams HSTR1-B

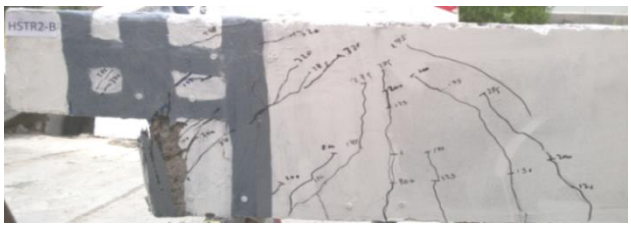

Figure 20 Cracks patterns for strengthening beams HSTR2-B

3.6 Specimens NSTR1-A & NSTR2-A

These specimens were strengthened with L-Shaped CFRP sheets at bottom faces of half joint; the NSTR2-A has the same strengthening configuration as the NSTR-1A, with adding two strips in horizontal direction at each face of half joint to increase shear strength at the re-entrant corner.

Comparing the load-deflection curve of these specimens against the specimen NCONT-A, it can be seen, that the ultimate load capacity is improved by about 2.7% and 10%, respectively, and the deflection is decreased by about 23% and 34%, respectively, as shown in Figure 21.

Figure 22 and 23 show the cracking history at failure for the two specimens respectively. Based on the mode of failure for the control specimen NCON-A, and putting in mind that the first crack is of the shear type at the re-entrant corner, the first arrangement of strengthening (L-shaped) was proposed. The goal of this configuration is checking whether the L-shaped CFRP sheet installation is efficient to be adopted. It can be seen that for specimen NSTR1-A that the first crack initiated at the re-entrant corner with load level of 35 kN as diagonal shear type and the flexural crack at 75 kN. The test was terminated by rupture due to direct shear at load level of 185 kN.

For specimen NSRT2-A, it can be seen that stiffness of the beam and the failure load were enhanced noticeably. The first diagonal crack at the re-entrant corner was due to the combined action of shear and moment developed at 50 kN followed by the flexural crack by 80 kN. Failure occurred by delamination of CFRP sheet at load of 200 kN. It can be concluded that with more bond length, better ultimate load may be obtained. The first shear crack (at re-entrant corner) appeared at a load level of 100 kN in comparison with 50 kN for NCONT-A. While the first flexural crack developed at a load, level of 75 kN, which is close to that of NSTR2-A, 80 kN.

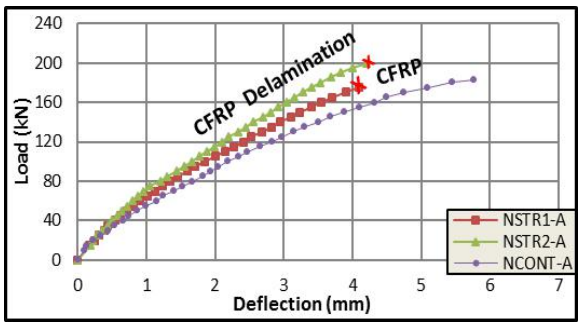

Figure 21 Effect of strengthening of nib region (a/d=1.5)

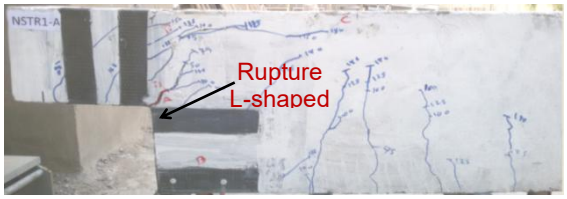

Figure 22 Cracks patterns for strengthening beams NSTR1-A

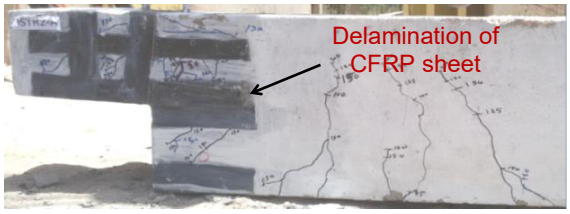

Figure 23 Cracks patterns for strengthening beams NSTR2-A

Shear failure is observed of the L-shaped CFRP sheets for specimen NSTR1-A. However, with adding the horizontal strips at the nib, Figure 23, more stiff behavior has been achieved and some development in ultimate load. Specimen NSTR1-B continues to accommodate loading up to the instant when bond failure between the epoxy and concrete occurred. Thus, one may conclude that using more layers of the L-shaped and the horizontal strips may results in increasing load capacity considerably.

3.7 Specimens NSTR1-B & NSTR2-B

For the shear slenderness ratio of (a/d=1), two specimens were strengthened at nib with modified strengthening configurations different from specimens NSTR1-A & NSTR2-A. The specimen NSTR1-B has been strengthened with three strips extended to include all the D-region. For specimen NSRT2-B, the strengthening scheme has been composed of the orthogonal and inclined strips. Moreover, the strengthened region was extended beyond the point of load application by 150 mm. Comparing the load deflection-curve of such specimens with specimen NCONT-B, it is obvious that the load capacity increased by about (13.56% and 15%), respectively. Stiffer response can be achieved, and the deflection

is decreased by about 22.06% and 39.3%, respectively, as shown in Figure 24.

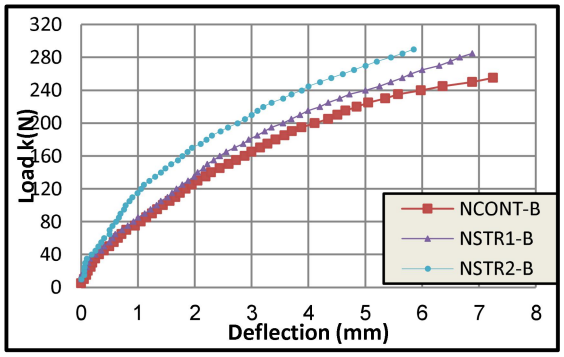

Figure 24 Effect of strengthening of nib region (a/d=1.0)

It can be concluded the failure mode for the both specimens is determined by a control factor, which is the lack of shear resistance in "deep beam action zone." Thus, it is expected that the load capacity of the beam may be developed noticeably if enough stirrups are provided at this zone. Also, it is observed that no cracks are developed at the half joint region for beams NSTR1-B & NSTR2-B up to failure, which is the goal of this study, as shown in Figures 23 and 24. CFRP restrict the growth of cracking close to the re-entrant corner. Thus, cracks shifted with higher rate than in specimen NSTR1-A away from the strengthened zone. Then, failure occurred by a diagonal shear failure.

Comparing crack patterns of the upgraded specimens, Figures 25 and 26, with that of specimen NCONT-B, it can be seen almost few cracks in the extended end of dapped beam. Moreover, the mode of failure is changed to diagonal shear failure at mid span of the beam whereas diagonal tension failure has been observed in the extended end for beam NCONT-B and cracks did not penetrate through CFRP sheet from the loading point towards the far support.

Figure 25 Cracks patterns for strengthening beams NSTR1-B

Table 4 shows that the first shear crack occurred before the flexural type for specimen NSTR2-A while the reverse can be seen for specimen NSTR2-B.

Figure 26 Cracks patterns for strengthening beams NSTR2-B

This may be explained that with higher a/d value, the re-entrant corner will be relatively weak zone. Thus, the first crack initiated from the corner at load level (as observed) of 50 kN. Then, flexural crack occur at load level of 80 kN. For specimen NSTR2-B, the stiffer zone due to strengthening and the smaller a/d value caused shifting of cracks out of the strengthened zone and the re-entrant corner. The first crack was flexural and developed at mid span (under the point load directly) within load of 75 kN. With further loading, the first shear crack occurred at level of 100 kN across the deep beam region. Stagnation of cracking occurred within the half joint without shifting to the far side, as it can accommodate more stresses up to failure at 300 kN which occurred by diagonal shear mode compared with specimen NSTR2-A which failed by bond failure of the vertical CFRP strip.

It can be seen that the first crack developed out of the strengthened zone as a flexural crack and most of cracks shifted to the far side of the beam. Diagonal crack developed at load level of 70 kN within the zone of deep beam action. This crack penetrated rapidly causing failure as in deep beams. It is expected that if the deep beam region was design adequately, more failure load may be obtained of 150/80 ratio. The above expression emphasizes the efficiency of the strengthening scheme to retire the lack of nib reinforcement of the dapped ends and half joints.

3.8 Effective Stiffness and Ductility

In the present work, the "effective stiffness" which is based on the strength at service load stage (0.75*Pu) have been adopted. Hence, the effective stiffness, Figure 27, may be expressed as:

$$K_e=(P_1/\Delta_1) \qquad (1)$$

Moreover, toughness is a measure of ability of a member to adsorb deformations before failure, or it is the dissipated energy caused by member deterioration up to failure, which is the area under the load deflection curve.

The ductility ratio is a measure for the ability of a member to deform beyond the yielding point or it is indicator for the warnings appear on the member before full collapse. Several proposals have been

suggested when the level at which steel yields is not known. Two suggestions have been adopted in the present work. One is based on the dissipation of energy (DI1) and can be expressed as follows, Figure 28:

$$\mu=0.5((E_t/E_e)+1) \quad (2)$$

In which Et: is the total energy dissipated up to failure; Ee: is the energy that proposed to be dissipated within the elastic stage (area of the hatched triangle).

The second method (DI2) to determine ductility is based on seeking for the point of intersection for the line that represent the initial stiffness with that representing stiffness at final stage of loading (displacement ductility), as shown in Figure 29. Thus, ductility ratio can be expressed as:

$$\mu=\Delta_{max}/\Delta_y \quad (3)$$

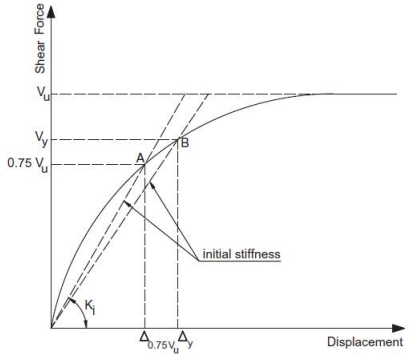

Figure 27 Effective stiffness determination [34]

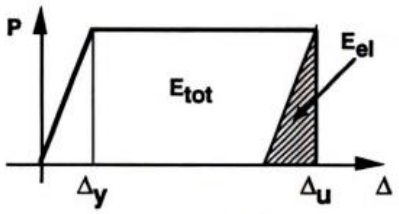

Figure 28 determination of ductility ratio by dissipated energy method [35]

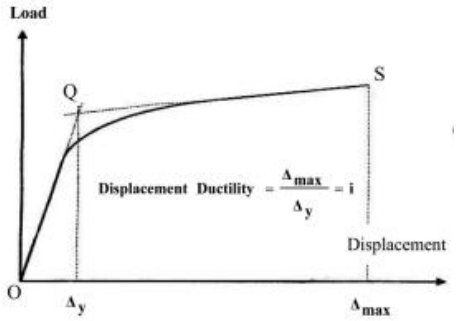

Figure 29 determination of ductility ratio by displacement method [36]

Figure 30 shows the effective stiffness values for the tested half joints. It can be seen that the useful (effective) stiffness increases with reducing a/d ratio. Furthermore, it can be observed that stiffness for specimen NCONT-A is slightly higher that the specimen CONT-A. This may be attributed to shifting the failure to the region of full depth rather than being occur in the extended end. Moreover, it is clear that the inclined configuration of strengthening (HSTR1-A) yielded better results and that the arrangement NSTR2-A may be adopted in strengthening the deficient nib end with a/d=1.5 unless that the arrangement NSTR2-B shows better results.

For a/d=1.0, it can be seen that arrangement HSTR1-B, (inclined configuration) yielded higher stiffness. For nib end strengthening, the configuration NSTR2-B, yield better performance. Thus, it is recommended to carry out further tests to check the adequacy of the arrangement NSTR2-B to be applied for half joint deficiently reinforced at nib end with a/d=1.5.

Figure 31 shows the ductility ratios calculated for the tested half joints based on Equations (2) (DI1) and (3) (DI2). It can be seen from Equation (1) that the ratio of the total to the elastic energy makes the expression not very sensitive to the stage of loading at which failure occurs. This can be seen for specimens NSTR1-A and NSTR2-A which failed at early stages compared to other specimens.

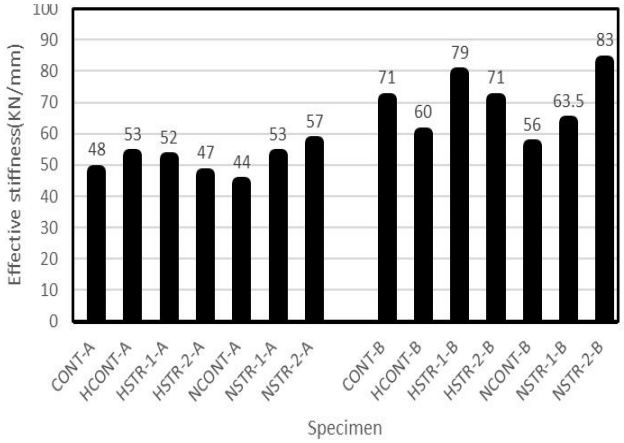

Figure 30 Effective stiffness values for the tested specimens

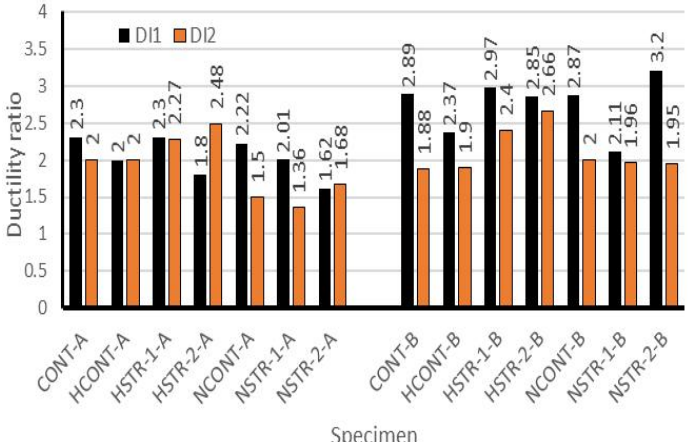

Figure 31 values of the ductility ratio for the tested specimens

In contrast, Equation (3) is affected by the value of maximum deflection that specimen yielded. Hence, it seems that Equation (3) yielded more acceptable and reasonable results. Furthermore, it can be seen that the ductility ratio increases with reducing a/d ratio.

4.0 CONCLUSION

It found that a/d ratio has a noticeable effect on behavior of the reinforced concrete half joints. For the reference specimens (the designed reinforcement), the reduction of shear slenderness ratio from 1.5 to 1.0, resulted in enhancement in the maximum load by about 17% and the mechanism of failure was found to be of the diagonal tension in the nib end instead of the diagonal tension in the re-entrant corner. The lack in stirrups provided in hanger by about 50%, yielded a reduction in beam capacity of about 13% regardless of shear slenderness ratio. Meanwhile, the reduction of tension steel at nib by about 60%, led to a drop in load capacity of about 56% for a/d=1.5 and 15% for a/d=1.0.

In addition, it is found that strengthening the nib region with an appropriate arrangement of CFRP strips resulted in initiation of first cracking with higher loading if compared with those non-strengthened specimens. The failure is shifted to occur beyond the point of loading, within the zone that has no shear reinforcement. The crack developed with orientation that is similar to the diagonal crack in deep beams.

In addition, it was found that using CFRP composites in upgrading RC half joint led to improvement in both the shear resistance and the general response of the half joint. The enhancement in the capacity for specimens upgraded at hanger regions with inclined aligned strips for shear slenderness ratio a/d of 1.5 and 1.0 is 17% and 23% respectively, and for specimens strengthened with vertical alignment is about 11% for shear slenderness ratio of 1.5 and 18% for ratio of 1.0. Furthermore, the enhancement in strength capacity for specimen strengthened at nib region with a/d =1.5 is about 10% for L-shaped alignment with horizontal strips. While the enhancement for a/d =1.0 with inclined alignment is about 15%. It is obvious that strengthening with CFRP sheet is an adequate technique to retire the strength drop due to lack in reinforcement in the disturbed zone (nib end and hanger) of a half joint and that the orientations of CFRP strips, has a noticeable influence in improvement the capacity. Thus, it is recommended to use the inclined 45° with mesh of horizontal and vertical strips at disturbed region. It is expected that such configuration may yield better results in comparison with other configurations of strengthening. Results shows also, that the effective stiffness and ductility ratio increase with reducing a/d value. In addition, it is observed that prediction of ductility ratio using Equation (3) is more adoptable for the fully reinforced, deficiently reinforced and the upgraded half-joints.

References

[1] S. K. Liem. 1983. Maximum Shear Strength of Dapped-end or Corbel. MSc Thesis. University Concordia. Montreal. Quebec. Canada.

[2] K.-H. Yang, A. F., Ashour and J.-K. Lee. 2011. Shear Strength of Reinforced Concrete Dapped-end Beams using Mechanism Analysis. The University of Bradford Institutional Repository. 1-38.

[3] Lu W.-Y., T.-C., Chen, and I.-J., Lin. 2015. Shear Strength of Reinforced Concrete Dapped-end Beams with Shear Span-to-Depth Ratios Larger than Unity. *Journal of Marine Science and Technology*. 23(4).

[4] ACI Committee 318M-2019. Building Code Requirements for Structural Concrete (ACI 318M-19) and Commentary (ACI 318M R-19). ACI, Farmington Hills, MI, USA.

[5] A. Atta and M. Taman. 2016. Innovative Method for Strengthening Dapped-end Beams Using an External Prestressing Technique. *Materials and Structures*. 49: 3005-3019.

[6] A. H., Mattock, and T. C., Chan. 1979. Design and Behavior of Dapped End Beams. *PCI Journal*. November-December. 24(6): 28-45.

[7] A. H. Mattock. K. C. Chen, and K. Soongswang. 1976. The Behavior of Reinforced Concrete Corbels. *Journal of Pre-Stressed Concrete Int*. 53-77.

[8] T. Peng. 2009. Influence of Detailing on Response of Dapped End Beams. M. Sc. Thesis. McGill University. Montréal, Canada.

[9] D. L., Barton, R. B., Anderson A. Bouadi, J. O. Jirsa and J. E. Breen. 1991. An Investigation of Strut-and-Tie Models for Dapped Beam Details. Research Report Number 1127-1. 187.

[10] W.-Y.Lu, I.-J., Lin and H.-W. Yu. 2012. Behavior of Reinforced Concrete Dapped-end Beams. *Magazine of Concrete Research*. 64(9): 793-805.

[11] M. Aswin, B. S., Mohammed, M. S., Liew, and Z. I., Syed. 2015. Shear Failure of RC Dapped-end Beams. *Journal of Advances in Materials Science and Engineering*. Publishing Corporation.

[12] R. N., Mohamed, K. S., Elliott. 2008. Shear Strength of Short Recess Precast Dapped End Beams Made of Steel Fibre Self-compacting Concrete. *33rd Conference on Our World In Concrete & Structures, Singapore*. 25-27.

[13] B. S. Mohammed, M. Aswin, M. S. Liew and N. Zawawi. 2019. Structural Performance of RC and R-ECC Dapped-End Beams Based on the Role of Hanger or Diagonal Reinforcements Combined by ECC. *Int J. Concr Struct Mater*. 13-44.

[14] S. Ahmad, A., Elahi, J., Hafeez, M. Fawad and Z. Ahsan. 2013. Evaluation of the Shear Strength of Dapped Ended Beam. *Life Science Journal*. 10(3): 1038-1044.

[15] P. Desnerck, J. M. Lees, and C. T., Morley. 2018. Strut-and-tie Models for Deteriorated Reinforced Concrete Half-joints. *Engineering Structures*. 161: 41-54.

[16] J. M. Falcon, L., Pallares and P. F. Miguel. 2019. Proposal and Experimental Validation of Simplified Strut-and-Tie Models on Dapped-End Beams. *Engineering Structures*. 183: 594-609.

[17] M. P., Werner, and W. H. 1973. Dilger, Shear Design of Prestressed Concrete Stepped Beams. *PCI Journal*. 18(4): 33-49.

[18] A. H. Mattock, and T. S., Theryo. 2009. Strength of Precast Prestressed Concrete Members with Dapped Ends. *PCI Journal*. 1986. 31(5): 58-75.

[19] A., Nanni and P.-C., Huang. 2002. Validation of an Alternative Reinforcing Detail for the Dapped Ends of Double Prestressed Tees. *PCI Journal*. January-February, 38-49.

[20] Amir, W. *et al*. 2017. Dapped Ends of Prestressed Concrete Thin-stemmed Members. *PCI Journal.* March–April.
[21] A. W, Botros, G. J., Klein, G. W.Lucier, S. H., Rizkalla and P. Zia. 2017. Dapped Ends of Prestressed Concrete Thin-stemmed Members, Part 1, Experimental Testing and Behavior. *PCI Journal.* March-April.
[22] P. C, Huang, J. J Myers and A. Nanni. 2000. Dapped-end Strengthening in Precast Prestressed Concrete Double Tee Beams with FRP Composites. *Proc., 3rd Inter. Conf. on Advanced Composite Materials in Bridges and Structures,* Ottawa, Canada, 15-18, Aug. 545-552.
[23] S. F., Taher. 2005. Strengthening of Critically Designed Girders with Dapped Ends. *Structures & Buildings*. 158(2): 141-152.
[24] Nagy-György, G. Sas , A.C. Da˘escu , J. A. O. Barros , V. Stoian. 2012. Experimental and Numerical Assessment of the Effectiveness of FRP-based Strengthening Configurations for Dapped-end RC Beams. *Engineering Structures.* 44: 291-303.
[25] Q. M. Shakir and R. Alliwe. 2020. Upgrading of Deficient Disturbed Regions in Precast RC Beams with Near Surface Mounted (NSM) Steel Bars. *Journal of Materials and Engineering Structures.* 7(2).
[26] Iraqi Specification No. 5. 1984. Portland Cement. Baghdad.
[27] Iraqi Specification No. 45. 1984. Natural Sources for Gravel that is used in Concrete and Construction. Baghdad.
[28] EFNARC. 2002. Specification and Guidelines for Self-Compacting Concrete. Association House, 99, West Street, Farnham, Surrey, London, UK, February.
[29] ASTM C-494/C 494M–01. 2001. Standard Specification for Chemical Admixtures for Concrete. Annual Book of American Society for Testing and Materials.
[30] ASTM A 370-05 .2005. Standard Test Method and Definition for Mechanical Testing of Steel Products. Annual Book of ASTM Standards, 1(1), ASTM, Philadelphia, PA.
[31] Sika, SikaWrap-301 C. Technical Data Sheet. 16/1/2015 edition. Sika Corporation.
[32] Sika. Sikadur 330. Technical Data Sheet, 13/6/2006 edition Sika Corporation.
[33] The Assessment of Reinforced Concrete Half- Joints AM-STR-06007 June 2014 Transport Infrastructure Ireland (Tii) Publications.
[34] N. S. Vu, L.Bing, K. Beyer. 2014. Effective Stiffness of Reinforced Concrete Coupling Beams. *Engineering Structures.* 76: 371-382.
[35] A. Naaman and S.Jeong. 1995. Structural Ductility of Concrete Beams Prestressed with FRP Tendons. *Proc. Second Int. RILEM Symp. (FRPRCS- 2) Non-Metallic Concr. Struct.*, Ghent, Belgium. 379-86.
[36] M. Rakhshanimehr, M. R. Esfahani, M. R. Kianoush, B. A Mohammadzadeh, and S. R Mousavi. 2014. Flexural Ductility of Reinforced Concrete Beams with Lap-spliced Bars. Can. *J. Civ. Eng.* 41(7): 594-604.